INVESTIGATION OF THE PARAMETERS IN THE BOUNDARY PLASMA OF ASDEX BY MEANS OF A LANGMUIR PROBE

M. Lenoci, G. Haas

IPP III/113

July 1986

MAX-PLANCK-INSTITUT FÜR PLASMAPHYSIK

8046 GARCHING BEI MÜNCHEN

MAX-PLANCK-INSTITUT FÜR PLASMAPHYSIK

GARCHING BEI MÜNCHEN

INVESTIGATION OF THE PARAMETERS IN THE BOUNDARY PLASMA OF ASDEX BY MEANS OF A LANGMUIR PROBE

M. Lenoci, G. Haas

IPP III/113 July 1986

Die nachstehende Arbeit wurde im Rahmen des Vertrages zwischen dem Max-Planck-Institut für Plasmaphysik und der Europäischen Atomgemeinschaft über die Zusammenarbeit auf dem Gebiete der Plasmaphysik durchgeführt.

IPP III/113 M. Lenoci
G. Haas

INVESTIGATION OF THE PARAMETERS IN THE BOUNDARY PLASMA OF ASDEX BY MEANS OF A LANGMUIR PROBE

ABSTRACT

The electron temperature and density were routinely measured at the edge of the ASDEX main plasma by means of a fast moving triple probe which gives the saturation current and T_e on line.

These measurements were made in ohmically heated discharges and during neutral beam injection in order to study the radial dependence of the plasma parameters in the boundary layer and the effects of auxiliary heating on it.

During lower hybrid application we observed strong poloidal and toroidal deviations in the floating potential that inhibit the operation of a triple probe. To investigate these effects, we used double probes and floating potential measurements. The most important reason, but not the only one, for these floating potential inhomogeneities are changes in the electron temperature of typically 10 - 20 eV over a distance of a few milliseconds.

INVESTIGATION OF THE PARAMETERS IN THE BOUNDARY PLASMA OF ASDEX BY MEANS OF A LANGMUIR PROBE

M. Lenoci, G. Haas

1. INTRODUCTION

In this report we describe Langmuir probe measurements at the edge of the ASDEX main plasma.
A triple probe which gives the saturation current and temperature on line was used /1/. With a fast moving probe it is possible to obtain complete density and temperature profiles in a single shot.

The measurements were made in ohmically heated discharges and during application of NBI, LHRH and LHCD in order to investigate the radial dependence of the plasma parameters in the boundary layer and the effects of auxiliary heating on it.

2. TRIPLE PROBE THEORY

Before the measurments are described, a short review of the triple probe theory is given here.
The triple probe is realized by adding a third floating electrode in close proximity to a double probe to which a constant voltage is applied. Since not only the third tip is floating, but also the double probe, all three tips are negative with respect to the plasma potential. (In our case tip 2 is the less negative.) Starting from the equations for the current in a double probe and to a floating single electrode:

$$I = I_{eo} \exp\left[-\frac{e(V_{pl}-V_2)}{T_e}\right] - I_{io},$$

$$-I = I_{eo} \exp\left[-\frac{e(V_{pl}-V_1)}{T_e}\right] - I_{io},$$

$$0 = I_{eo} \exp\left[-\frac{e(V_{pl}-V_3)}{T_e}\right] - I_{io},$$

one readily obtains:

$$e(V_2-V_3) = T_e \left(\ln 2 - \ln\left(1 + \exp\left[-\frac{e(V_2-V_1)}{T_e}\right]\right)\right).$$

In the previous equations T_e is the electron temperature in eV, V_{pl} the plasma potential, I_{eo} the electron saturation current and I_{io} the ion saturation current.

If the constant voltage applied is $\geq 3\frac{T_e}{e}$, the current in the double probe is the saturation current I_{sat} and the potential difference between the most positive and the floating tip is proportional to the electron temperature.

The density is determined by means of the following formula:

$$n_e = \frac{I_{sat}}{e\sqrt{\frac{T_e}{2\pi\, m_i}}\; 2Q\sqrt{\pi}\; G_i},$$

where 2Q is the projected probe surface and G_i is a correction factor taking into account the influence of the magnetic field, which has to be determined experimentally. The triple probe, compared with double or single probes, has the advantage of a much higher time resolution since only a constant voltage instead of a sawtooth has to be applied. The saturation current and the temperature are given on line; with a fast radially moving triple probe, like the one installed in ASDEX, it is therefore possible to measure complete $n_e(r)$ and $T_e(r)$ profiles in one shot.

The only restriction associated with the use of the triple probe is that for its proper functioning the deviations between the floating potentials of the three tips must be small compared with $\frac{T_e}{e}$. In ohmic and NI discharges this condition is fulfilled, whereas during LH application we observed floating potential difference of the order of T_e/e, as described in Sect. 4.3.

3. DESCRIPTION OF THE EXPERIMENTAL ARRANGEMENT

The three tips of the probe are made of molybdenum, are 1 mm in diameter and 2.5 mm long and can easily be replaced; each tip has its own insulation

($Al_2 O_3$) and screen tube (Mo) and is at a distance of 7 mm from the other two. We also conducted exploratory experiments with smaller and larger distances (2 mm, 13 mm). The probe is mounted on a vacuum manipulator and can be moved from a preset position 100 mm radially inward and backward within 200 ms. This fast movement allows one to get very close to the separatrix without melting the tips. In ohmic discharges the separatrix can almost be reached, whereas in auxiliary-heated discharges the probe was kept 2 - 4 cm more outside in order to limit the heat load of the probe to a safe value.

The probe is placed 22.5^{o} toroidally away from the LH launching grill and 5^{o} poloidally above the equatorial plane.
The electric circuit used for the triple probe measurements is shown in Fig. 1. A constant voltage (150 V from a Kepco power supply) is applied between two tips of the probe. The saturation current is measured with a current probe, and the voltage by means of a divider and an isolation amplifier. The differential amplifiers are added to reduce the noise and the pick-up from the mains.

4. EXPERIMENTAL RESULTS

4.1 Ohmically heated discharges

Figure 2 shows for an ohmic discharge the ion saturation current and the potential difference ($\propto T_e$) collected with the triple probe moving from 12.5 cm to 3 cm outside the separatrix.
In Fig. 3 the results are compared with Thomson scattering measurements. In this case the separatrix intersects the equatorial plan at a major radius R = 202 cm. From such comparisons we derive the correction factor $G_i \simeq 1$.

Figures 4 and 5 show, respectively, Langmuir probe signals and the density and temperature profiles for an OH shot in which the probe, at the maximum elongation, is 1 cm from the separatrix.
From Fig. 5 the existence of three zones with different decay lengths for both T_e and n_e profiles is evident. Close to the separatrix $(r-r_s) < 2.3$ cm the decay length λ is short, then there is a region with larger λ ("plateau") and finally for $(r - r_s) > 5.5$ cm λ again becomes small. For n_e these findings are in agreement with Li-beam measurements /2/.

In Fig. 6 density profiles measured by the Li-beam diagnostic /2/ and by Langmuir probes are compared. All the data refer to the same shot and are taken at two plateaus in the main plasma density: $\bar{n}_e = 1.8 \times 10^{13}$ cm^{-3} and 3.2×10^{13} cm^{-3}. The shape of the profiles obtained by the two diagnostics is very similar; the shift in the absolute value ($\simeq$25 %) may be due to the errors in the calibration factors.

4.2 Neutral-beam-heated discharges

During the L-phase of neutral-beam-heated discharges a clear increase in the edge density was observed. The temperature increases, too, but by a smaller factor. Figure 7 shows density and temperature profiles between 7 and 3 cm outside the separatrix in the OH and L-phases for two discharges, both with the following parameters: He, $\bar{n}_e = 4.2 \times 10^{13}$ cm^{-3}, $B_t = 2.2$ T, $I_p = 380$ kA. There is practically no evidence of a change in the decay length during the L-phase with respect to the OH-phase.

The increase in density and temperature is a function of the NI-beam power as is shown in Fig. 8. The shots shown in Fig. 7 belong to the series analyzed for this power scan.

During the H-phase the saturation current is strongly modulated by ELMs like the H_α-signal in the divertor chamber (Fig. 9). In the following, we restrict ourselves to probe data collected during parts of the H-phase free of ELMs.

The ion saturation current ($\propto n_e \sqrt{T_e}$) and the temperature are plotted in Figs. 10 and 11, respectively, versus the radial position. These measurements were done during inward and outward movement of the probe in two shots with the following parameters:

D_2; $\bar{n}_e = 3.1 \times 10^{13}$ cm^{-3}; $B_T = 1.9$ T; $I_p = 320$ kA, $P_{NI} = 3.45$ MW,

showing good reproducibility and no difference between inward and outward movement.

In Fig. 12 we compare I_{sat} profiles from the OH,L,H (without ELMs) phases of shots belonging to this series.
From this figure it is seen that during the L-phase a significant increase

of the saturation current occurs, whereas the OH and the H-phases show similar I_{sat} profiles.

4.3 LH application

In the context of LH application it is worth mentioning that the probe is placed roughly 1 m from the LH grill in a magnetic flux bundle directly connected to the space in front of the RF coupler.
As already stated in Sect. 2, for proper functioning of triple probes it is necessary that the deviations between the floating potentials of the three tips be small compared with T_e/e. We investigated this effect for different plasma and LH parameters, as shown in Table 1.

Table 1

Series	LH		Plasma				Measurements
	Power (kW)	$n_{\parallel}$	B_T(T)	I_p(kA)	$n_e(cm^{-3})$	Species	
I	770	2	2.37	300	$1.4x10^{13}$	D_2	profiles of float.pot. diff.
II	750	2	"	"	$2.7x10^{13}$	"	" "
III	370	4	2.18	"	$2.1x10^{13}$	"	" "
IV	275	4	"	380	$2.7x10^{13}$	"	" "
V	500	2	"	300	$1.4x10^{13}$	"	" , I-V charact., combined double probes
VI	"	2	"	"	$2.9x10^{13}$	"	" "
VII	"	2	"	"	$1.4x10^{13}$	D_2+He	I-V charact., independent double probes
VIII	"	2	"	"	$2.9x10^{13}$	"	explorative, independent double probes

The floating potential differences were used to construct the electric field vector. The direction and absolute value of this show a strong radial dependence (Fig. 13, 14). Under the conditions of series I, II, V, VI we found a large component parallel to the magnetic field at the innermost radial position. At the radial position of the grill the absolute value of the vector is much smaller. Despite the different main plasma density in the series V and VI we found a very similar radial dependence of the direction. The same result

was obtained for the two series III and IV with lower RF power, for which the absolute value of the vector was always rather small. The reason for the deviations in floating potentials may be local inhomogeneities in the electron temperature or in the plasma potential or in the flux of suprathermal electrons. These can arise from effects connected with decay processes in between the grill and the separatrix, as described by, for example, Derfler /3/ and Motley and Glanz /4/.

In order to distinguish between these possible explanations, we operated for the series V, VI, VII and VIII couples of tips from the triple probe as double probes. The fast movement was modified in such a way that the probe stays for about 100 ms at the innermost position where the I-V characteristics were taken. In series V and VI we measured with two combined double probes with tip 3 as common reference tip. Under these conditions tip 3 has to carry the sum of the currents of tips 1 and 2, and from the characteristics one cannot find floating potential differences. They have to be measured independently. The characteristics (Fig. 15, 16) show only small differences between high and low main plasma density (corresponding to the ion-RF and the electron-RF interaction regimes, respectively) and indicate for couple 1-3 a lower temperature than for couple 2-3. This is in agreement with the direct floating potential measurements (Fig. 13,14), but not with the relative shift of the two characteristics.

For series VII with parameters like series V but with a changed plasma composition we increased the voltage range to 0 - 600 V in order to achieve saturation more readily. We used the two couples 1-3 and 2-3 alternatively and not connected. In this case we again find a lower temperature for the couple 1-3 than for couple 2-3 (Fig. 17) (67 and 80 eV, respectively). The floating potential difference can now be derived from the shift of the characteristics (30 V) and is within 30 % in agreement with the temperature difference.

In addition to this series VII in the electron regime, we also made some exploratory measurements in the ion regime but otherwise under the same conditions (series VIII). We again found no significant difference between high and low density. This may indicate that a plasma exists in between the LH grill and the separatrix that is dominated by the LH wave or by any decay waves and decoupled from the main plasma.

In other exploratory measurements we investigated for comparison purposes ohmically heated discharges with plasma parameters like series VI and VIII. We found much lower electron temperatures (15 eV instead of 65-80 eV) and higher electron densities (3×10^{12} instead of 1×10^{12} cm^{-3}) (Fig. 18). This is in agreement with mesurements done by Pericoli on FT /5/ and El Shaer on ASDEX /6/, who found a strong reduction of the density in front of the LH grill during RF application.

In conclusion, during LH application we observed strong poloidal and toroidal deviations in the floating potential. These deviations exist under all plasma and LH conditions investigated until now and can completely inhibit the operation of a triple probe. But other fast moving electrostatic probes may be disturbed, too, since the radial dependence of the floating potential differences acts like a temporal change of the probe potential which cannot be controlled. The most important reasons for these deviations are changes in the electron temperature of typically 10 - 20 eV over a distance of 7 mm. But some findings, such as an additional shift in the I-V characteristic or large components of the floating potential differences parallel to the magnetic field lines, cannot be explained by temperature differences. One has also to assume locally inhomogeneous fluxes of suprathermal electrons and differences in the plasma potential.

References:

/1/ S. L. Chen, T. Sekiguchi, J. Appl. Phys. 36, 2363 (1965).
M. Kamitsuma, S.L. Chen, J.S. Chang, J. Phys. D 10, 1065 (1977).

/2/ K. McCormick, Z.A. PLietrzyk, H. Murmann, M. Lenoci, et al., 7th PSI, Princeton, 1986, to be publ. in J. Nucl. Mat.

/3/ H. Derfler, private communication.

/4/ R. W. Motley, J. Glanz, Phys. Fluids 25, 2107 (1982).

/5/ V. Pericoli-Ridolfini, Plasma Phys. and Contr. Fus. 27, 709 (1985).

/6/ M. El Shaer, IPP Garching Report IPP III/96 (1984).

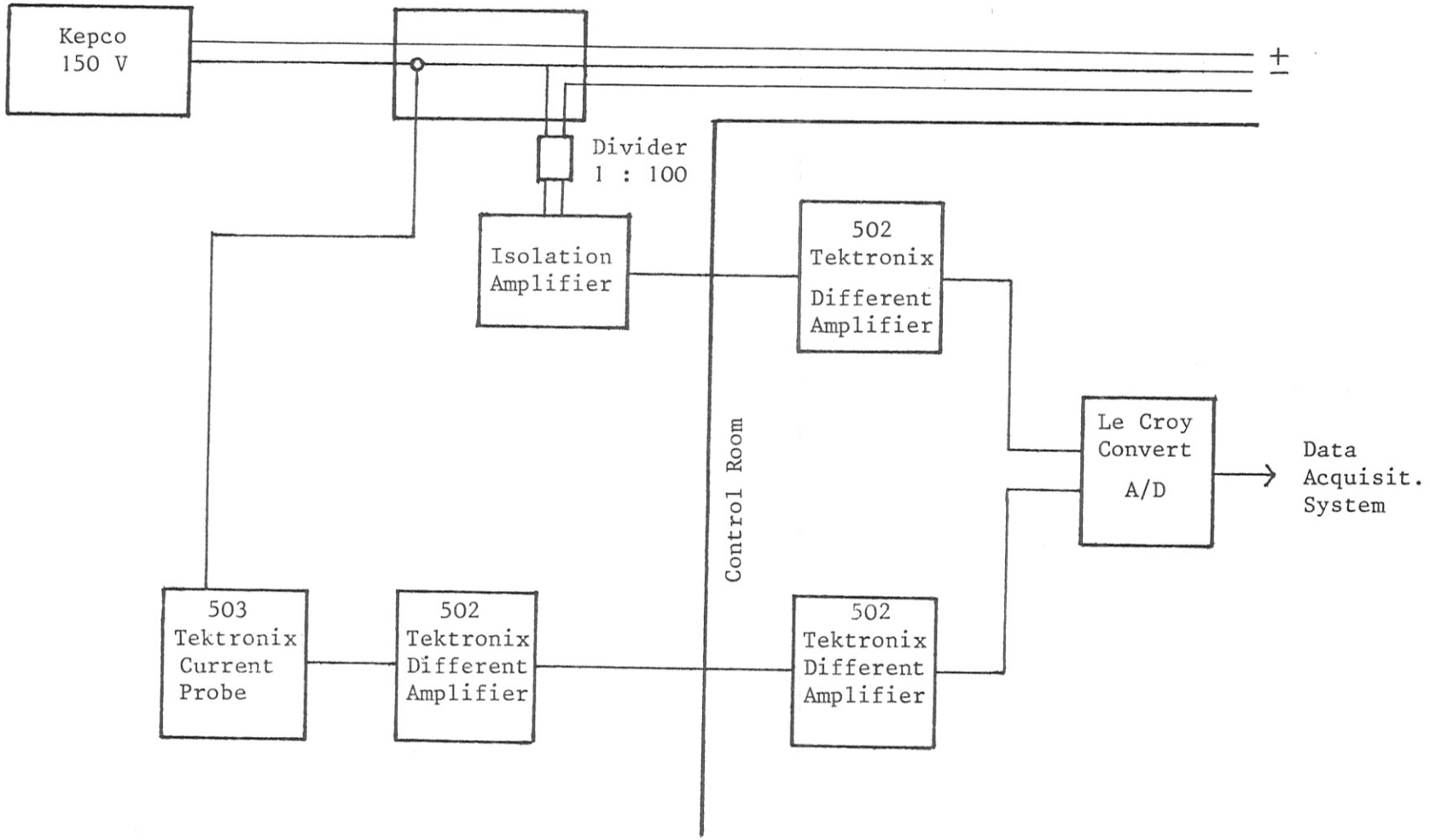

Fig. 1: Electric circuit used for triple probe measurements.

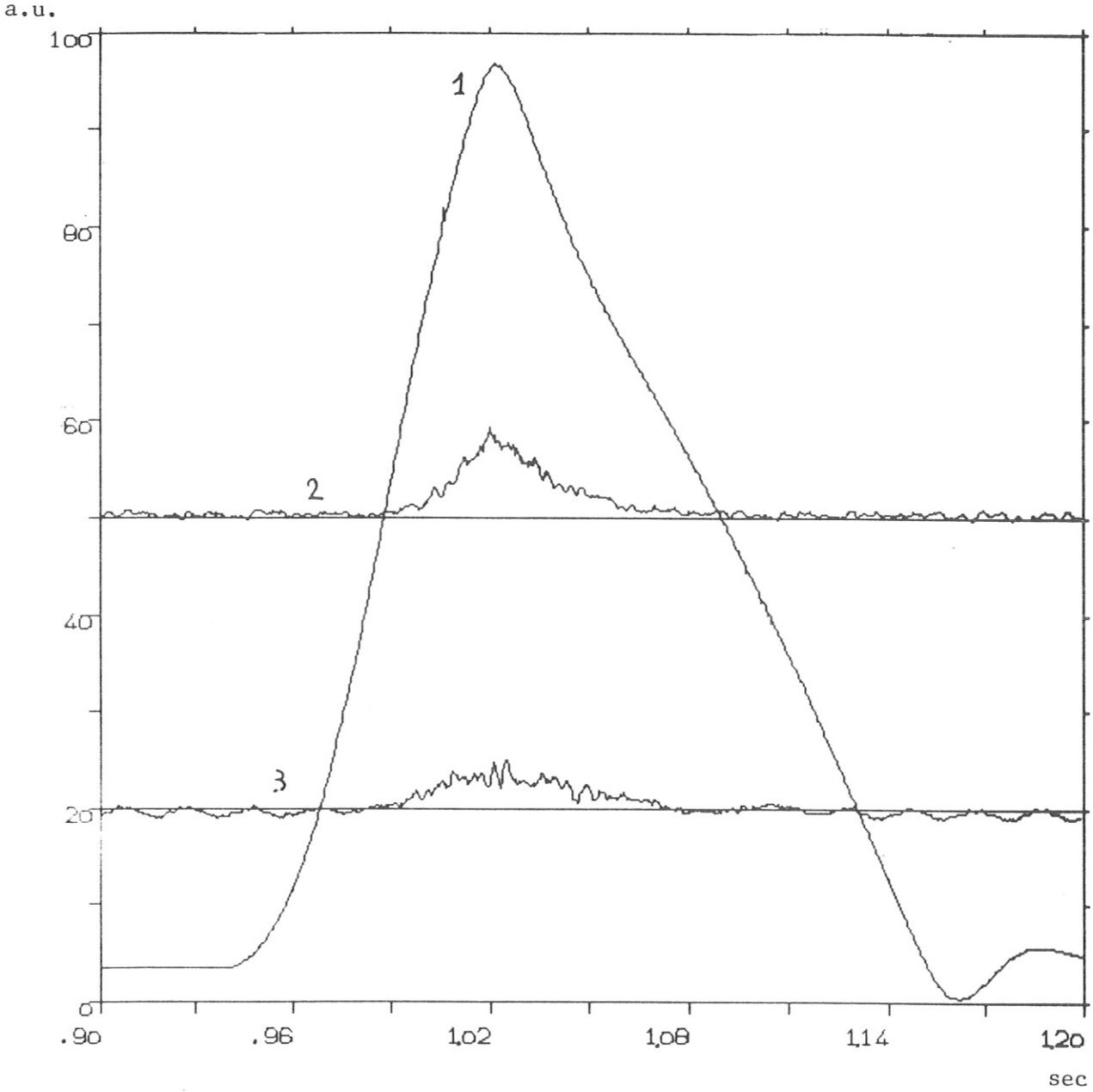

Datum	Schuss	Diagn.	Signal	Massstab	Mittl.	Unt.	I
01-AUG-85	16914	110	HUBH	-0.5000E+01	0	0.0	
01-AUG-85	16914	110	UH	-0.5000E+01	2	20.0	
01-AUG-85	16914	110	IH	0.5000E+01	2	50.0	

Fig. 2: Radial probe position (1) (fast movement), saturation current (2) and potential difference (3) ($\propto T_e$) from a triple probe measurement in an ohmic discharge.
H_2; $\bar{n}_e = 1.4 \times 10^{13}$ cm^{-3}, $I_p = 320$ kA; $B_T = 2.2$ T.

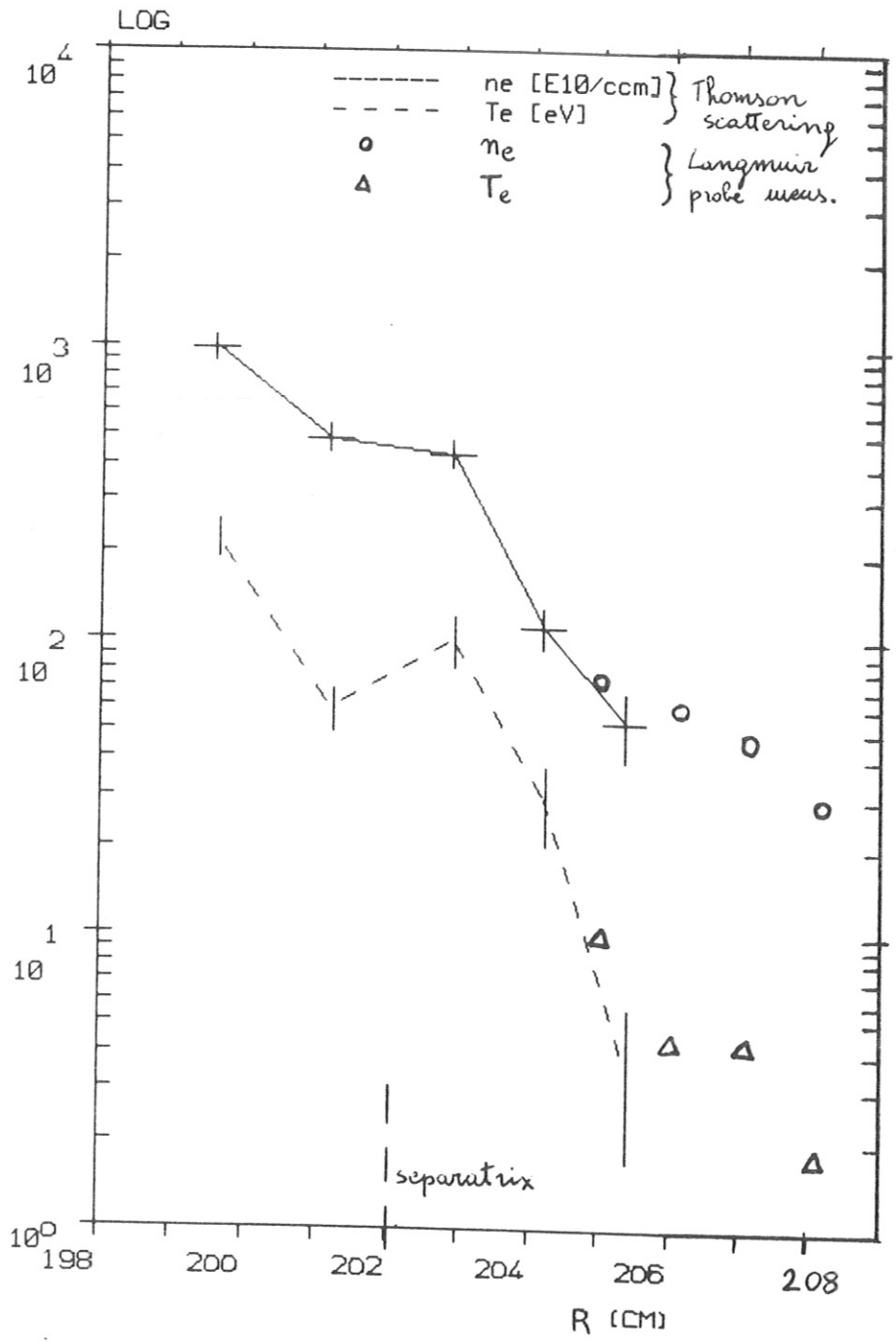

Fig. 3: Density and temperature radial profiles measured by Thomson scattering and Langmuir probe for the same shot as shown in Fig. 2.

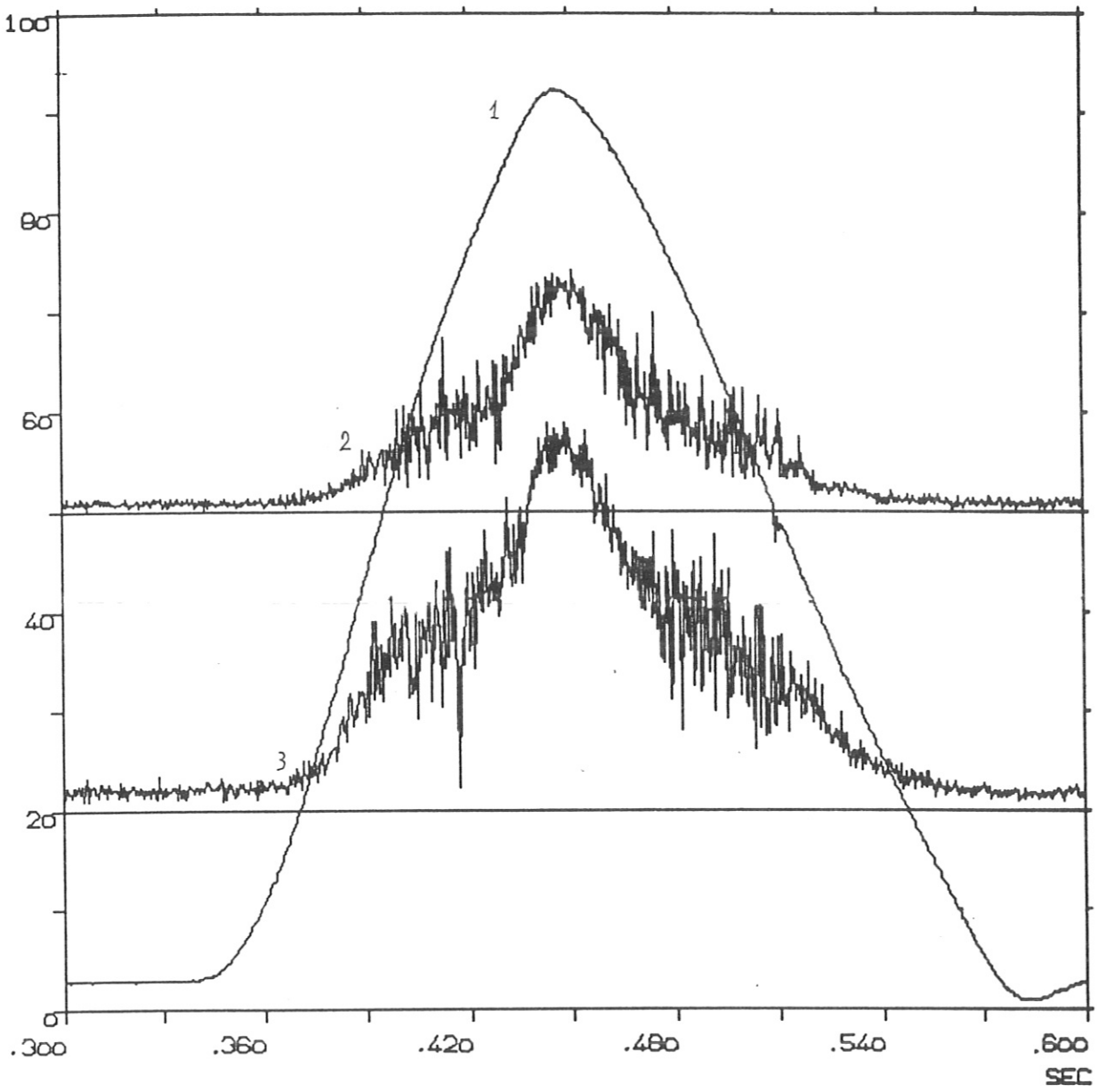

Datum	Schuss	Diagn.	Signal	Massstab	Mittl.	Unt.	I+ [A/V]
13-FEB-86	19358	110	UH	0.5000E+01	0	20.0	
13-FEB-86	19358	110	IH	0.5000E+01	0	50.0	
13-FEB-86	19358	110	HUBH	-0.5000E+01	0	0.0	

Fig. 4: (1) Radial probe position (fast movement), saturation current (2) and potential difference (3) ($\propto T_e$) from a triple probe measurement in an ohmic discharge
He, $\bar{n}_e = 4 \times 10^{13}$ cm^{-3}, $I_p = 320$ kA, $B_T = 2.2$ T

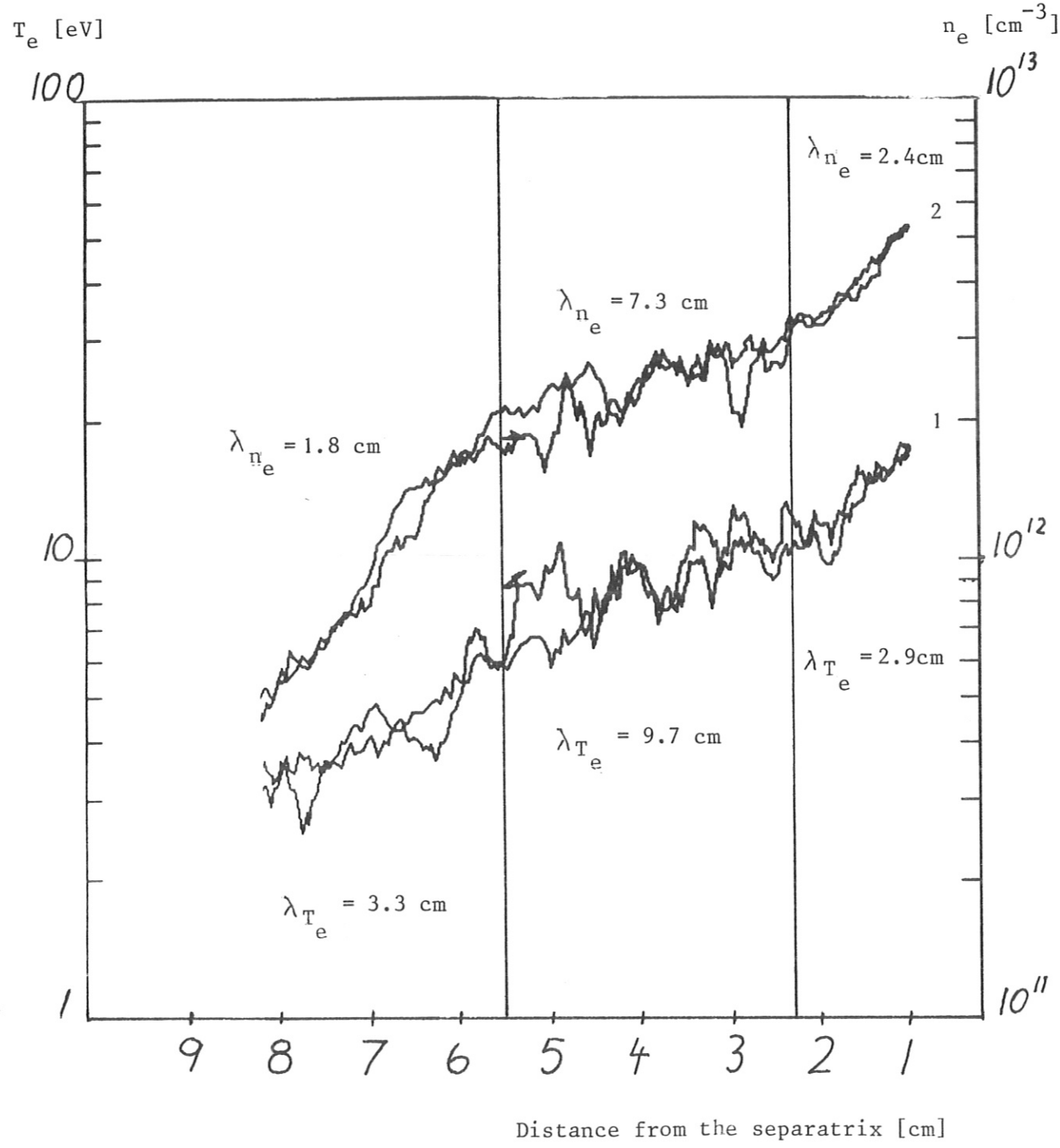

Fig. 5: Temperature (1) and density (2) radial profiles from Langmuir probe measurements for the same shot as shown in Fig. 4 (inward and outward movement).

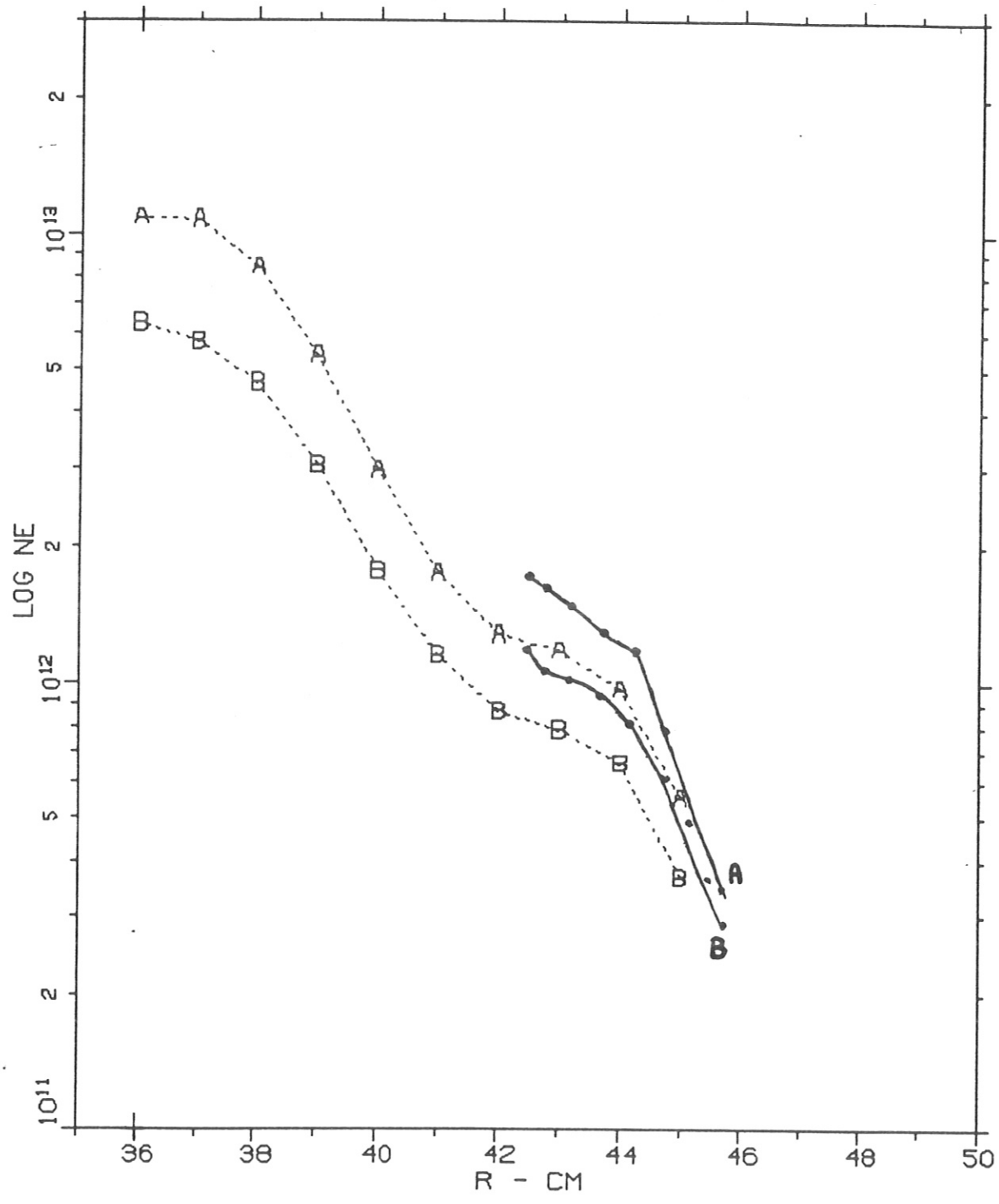

Fig. 6: Comparison of density profiles measured with Li beam diagnostic (dashed line) and Langmuir probes (full line) for two main plasma densities:

A: $\bar{n}_e = 3.2 \times 10^{13}$ cm^{-3}

B: $\bar{n}_e = 1.8 \times 10^{13}$ cm^{-3}

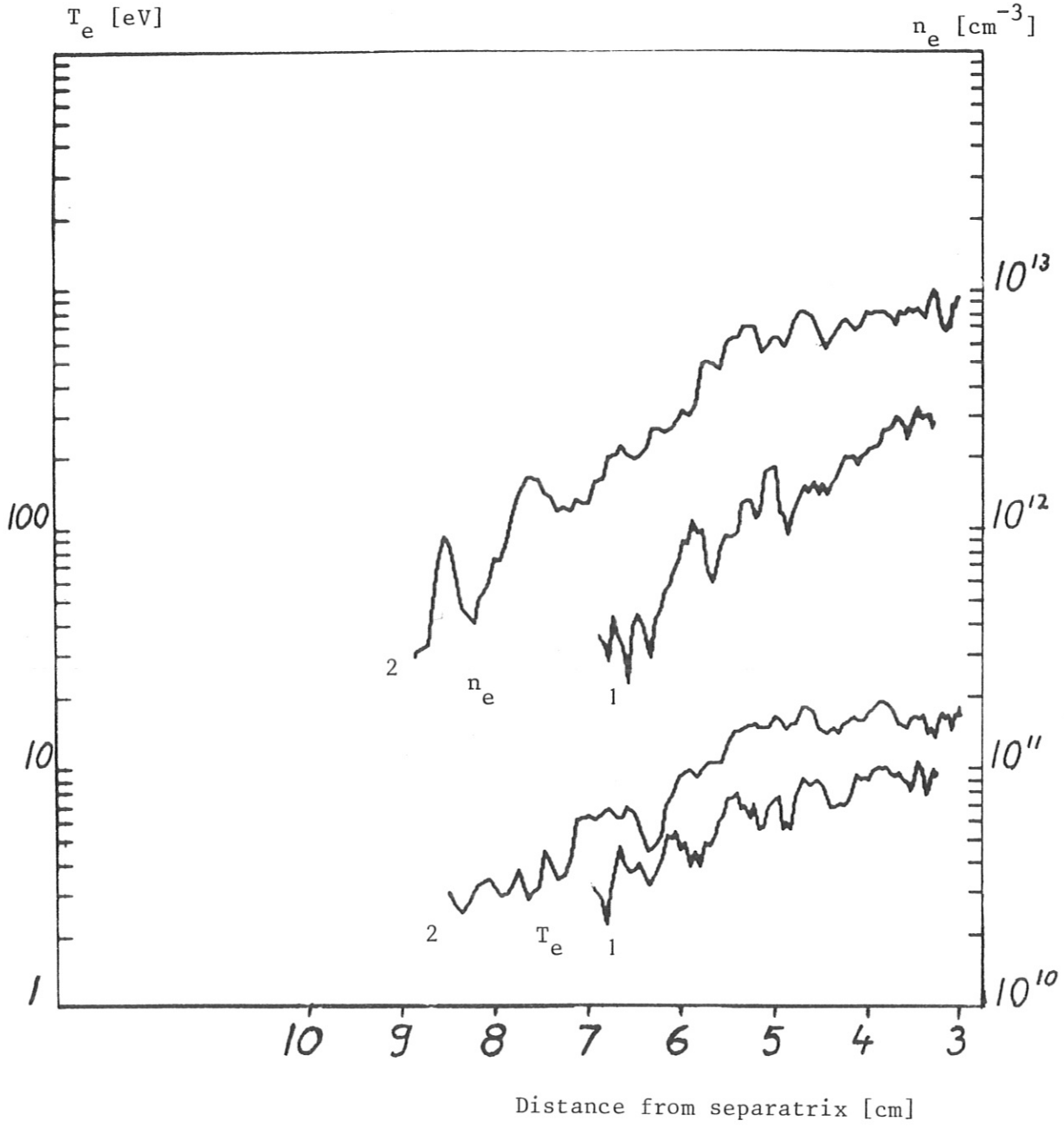

Fig. 7: Radial profiles of T_e and n_e for OH (1) and L (2) phases in He discharges
$\bar{n}_e = 4.2 \times 10^{13}$ cm^{-3}, I_p = 380 kA, B_t = 2.2 T, P_{NI} = 2.57 MW.

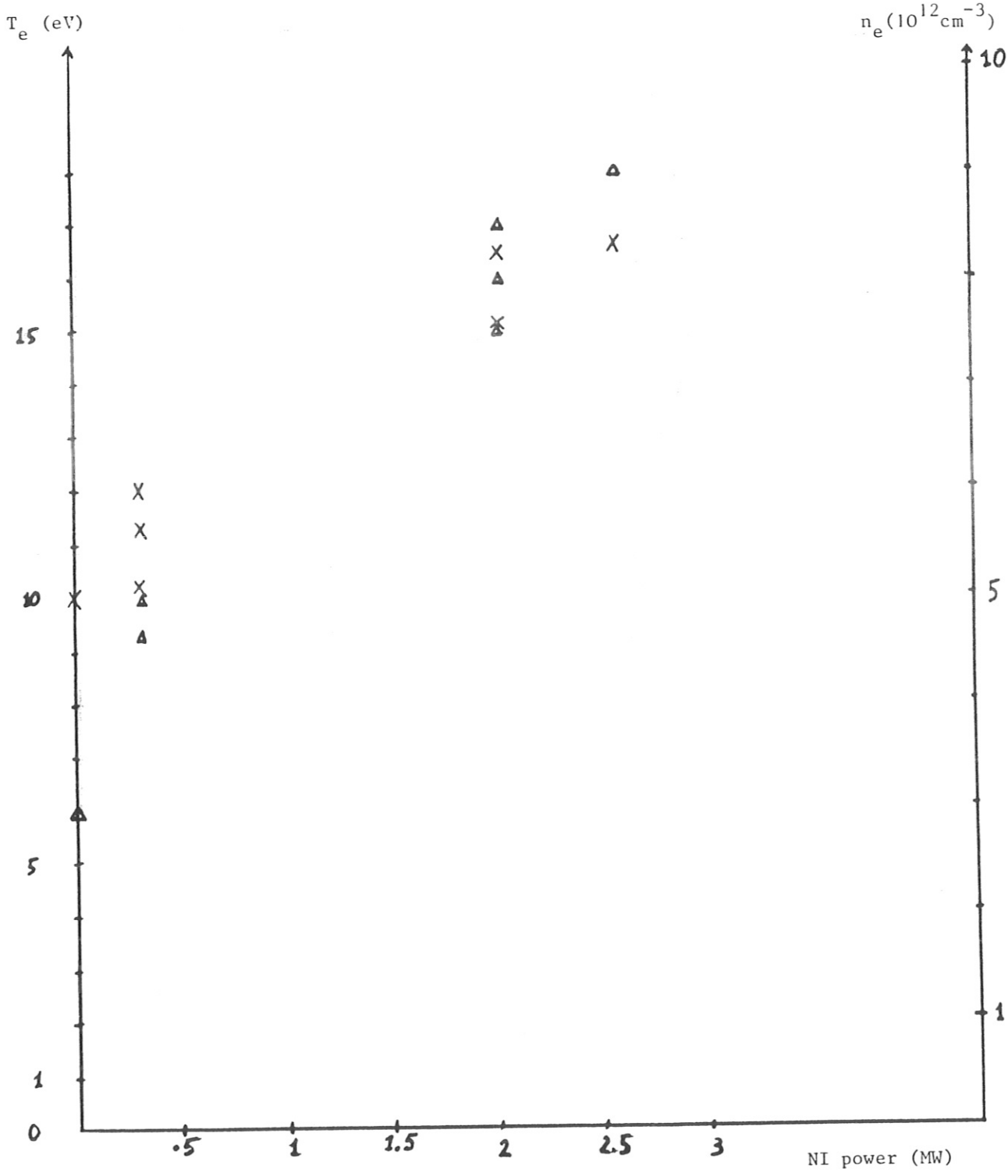

Fig. 8: Neutral injection power scan for shots in He.
$\bar{n}_e = 4.2 \times 10^{13}\ cm^{-3}$, $B_T = 2.2$ T, $I_p = 380$ kA
Δ: n_e, X: T_e at 3.7 cm outside the separatrix.

a.u.

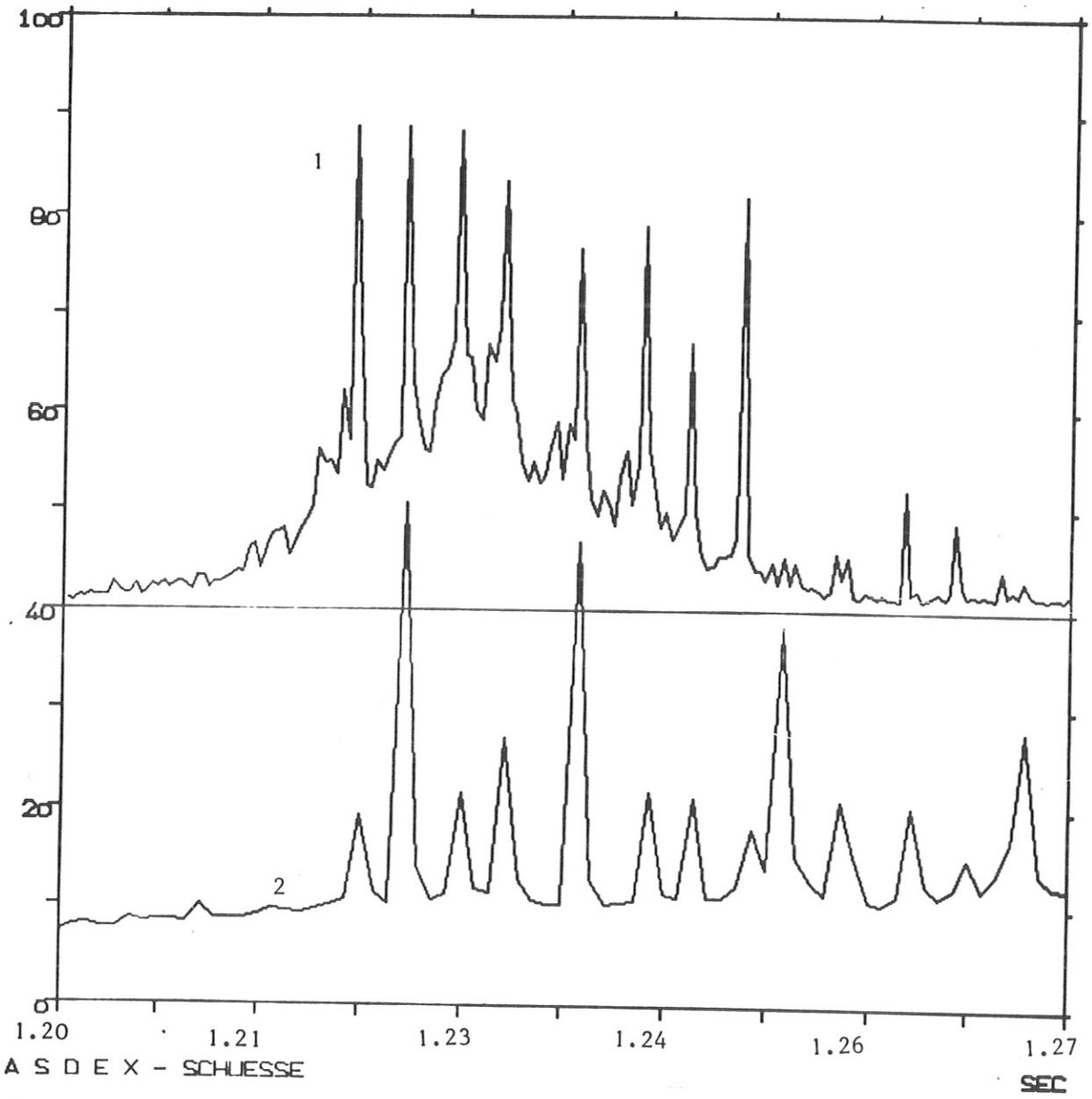

Fig. 9: Saturation current (1) and H_α signal (2) for a typical H-phase.

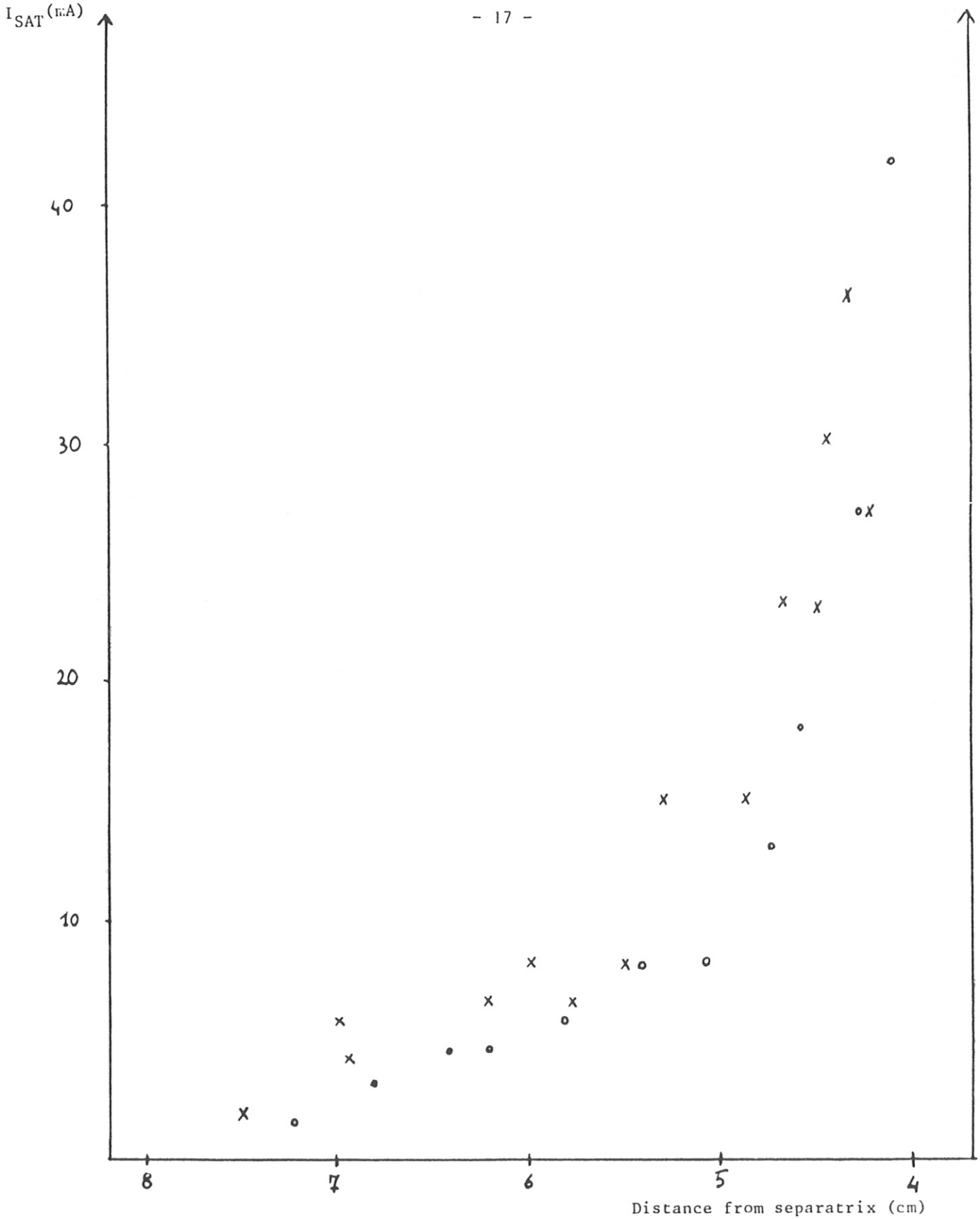

Fig. 10: Ion saturation current radial profiles during the H-phase free of ELMs.
D_2: $\bar{n}_e = 3.1 \times 10^{13}$ cm^{-3}; $B_T = 1.9$ T; $I_p = 320$ kA, $P_{NI} = 3.45$ MW
O : inward movement; x: outward movement

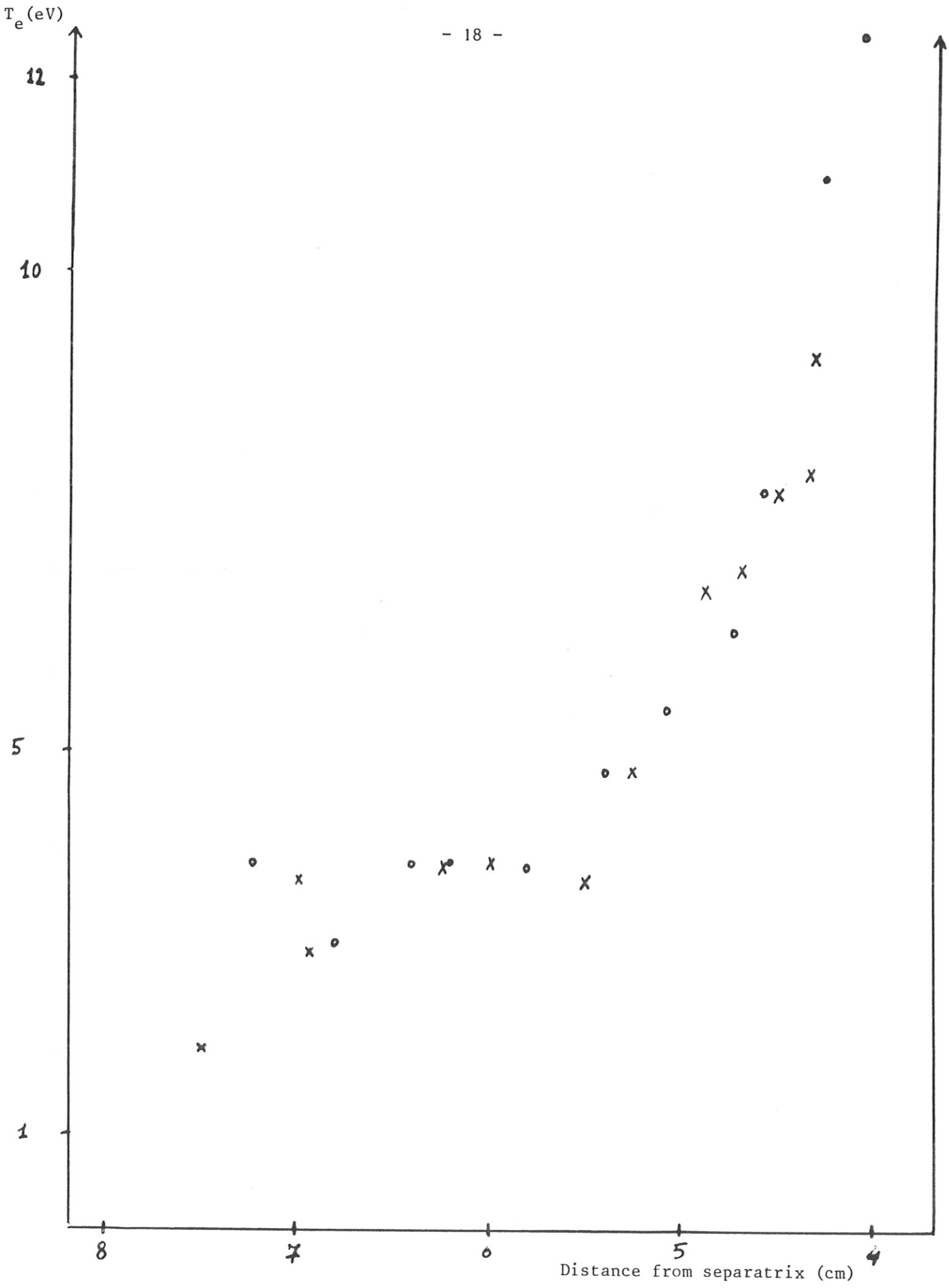

Fig. 11: Temperature radial profiles during the H-phase free of ELMs for the same shots as shown in Fig. 10.
O: inward movement; x: outward movement

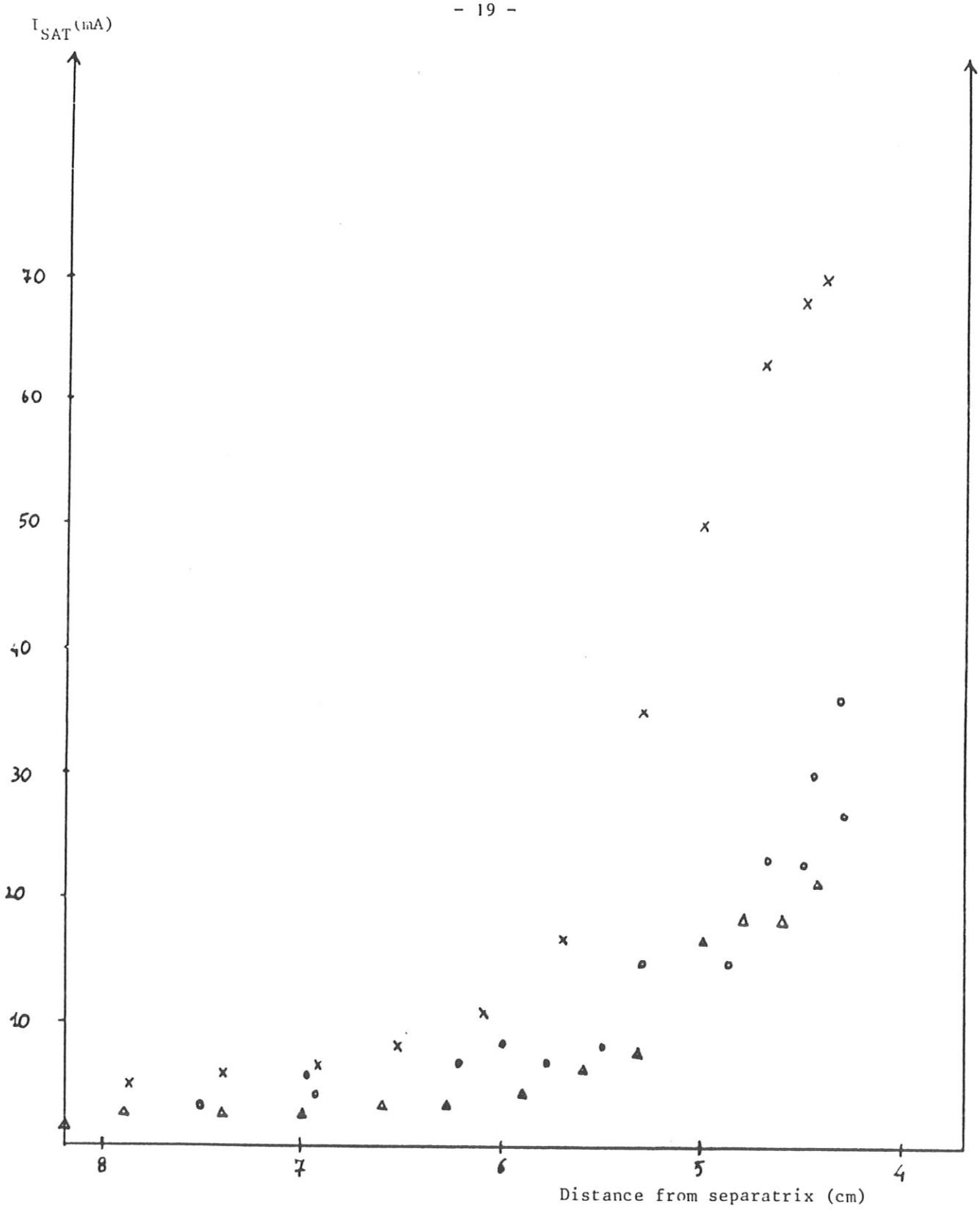

Fig. 12: Ion saturation current radial profiles in the three different phases of the same shot (# 18041)
Δ: OH phase x: L-phase O: H-phase without ELMs
D_2; $\bar{n}_e = 3.1 \times 10^{13}$ cm^{-3}; $B_T = 1.9$ T; $I_p = 320$ kA; $P_{NI} = 3.45$ MW.

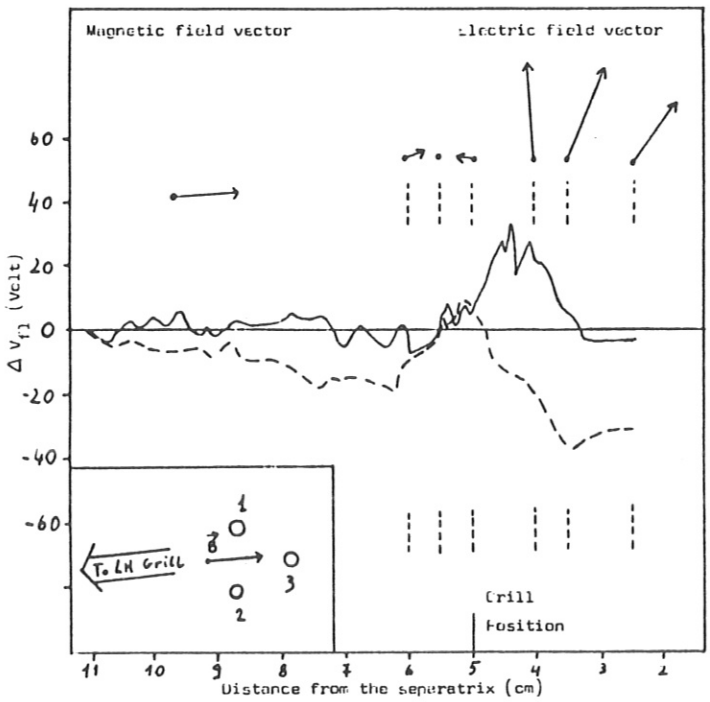

Fig. 13: Radial profiles of floating potential differences. SERIES VI
———— tips 1-3
-------- tips 2-3

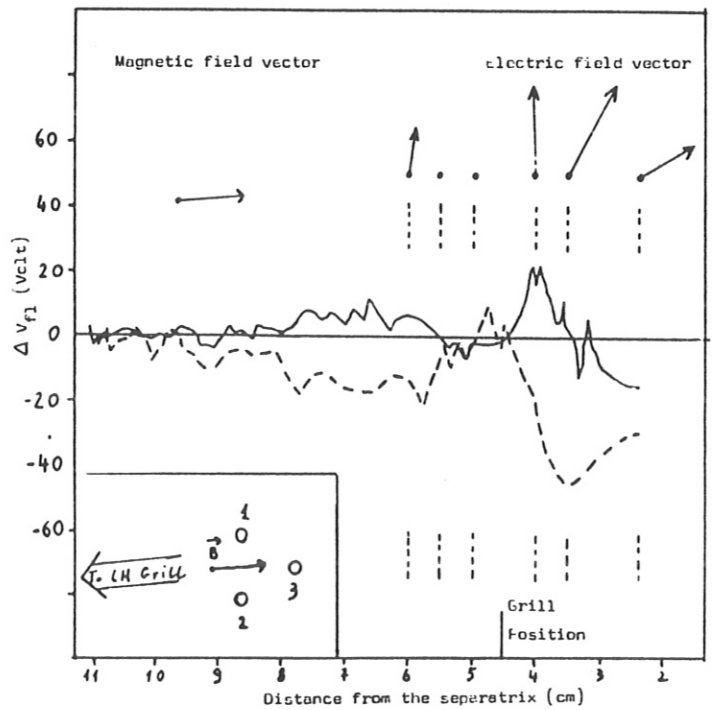

Fig. 14: Radial profiles of floating potential differences SERIES V

———— tips 1-3
-------- tips 2-3

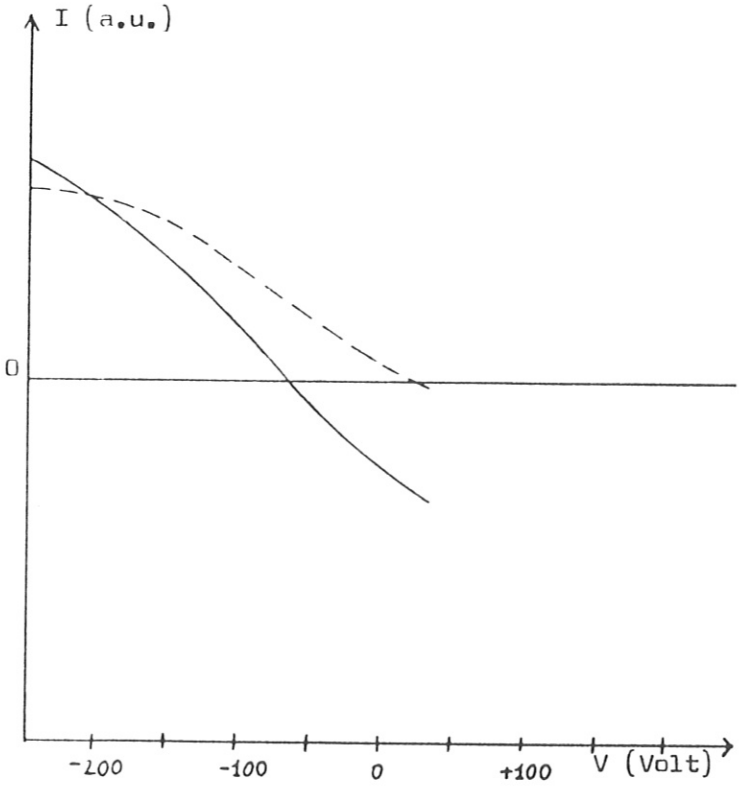

Fig. 15: I-V characteristics
SERIES VI
———— Tips 1-3
--------- Tips 2-3

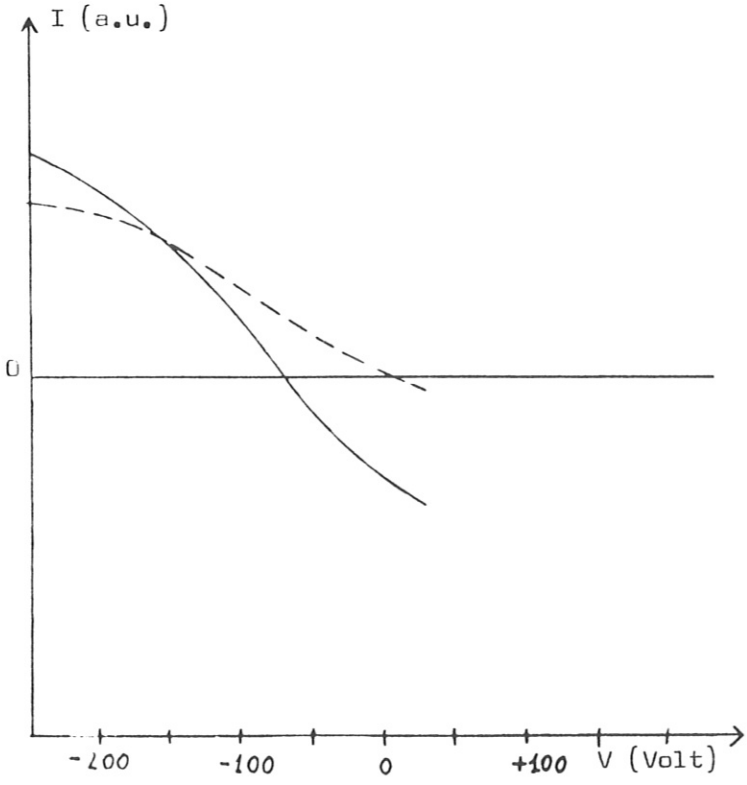

Fig. 16: I-V characteristics
SERIES V
———— Tips 1-3
-------- Tips 2-3

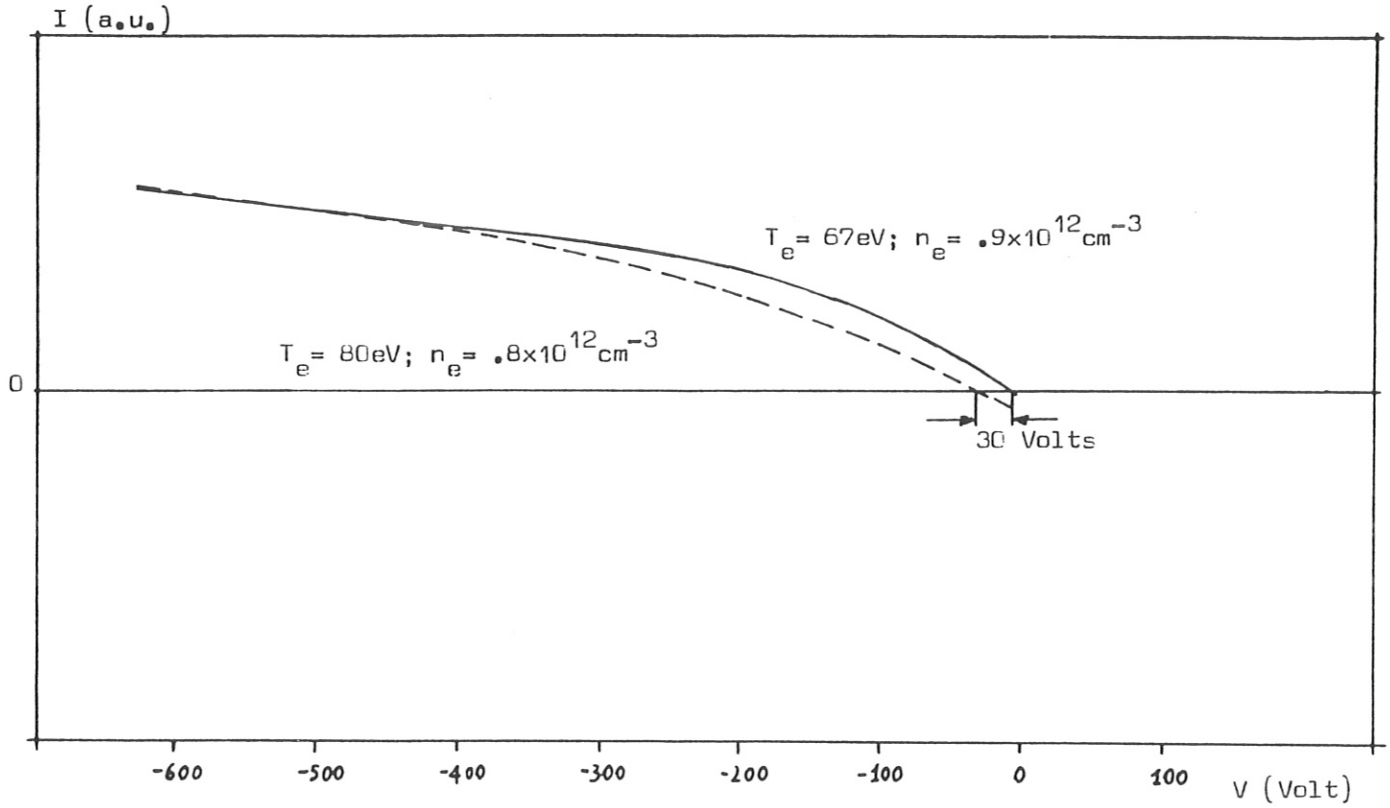

Fig. 17: I-V characteristics SERIES VII

———— Tips 1-3
---------- Tips 2-3

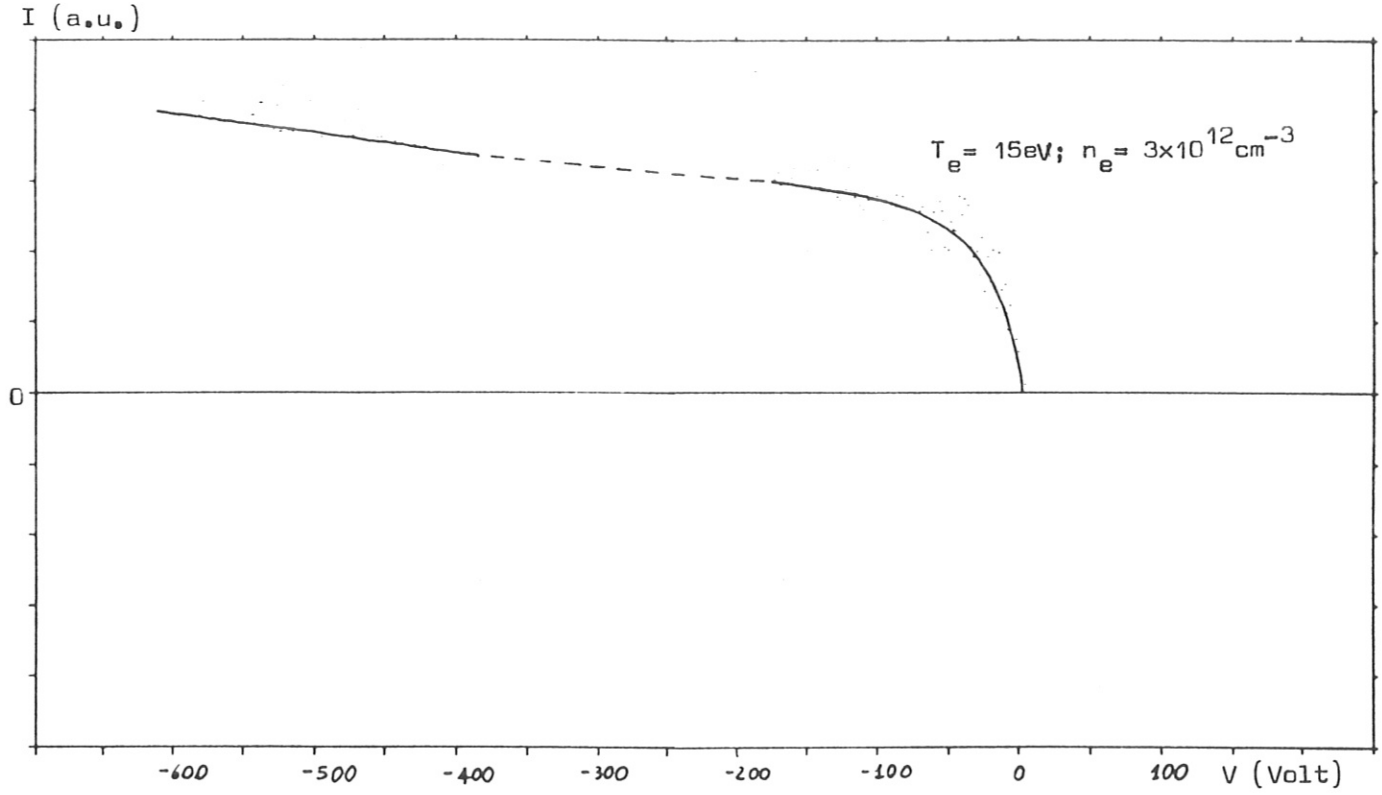

Fig. 18: I-V characteristics OH-discharge
$\bar{n}_e = 2.9 \times 10^{13}$ cm^{-3}